BALLISTIC IMPACT RESISTANCE

OF

FIBER-REINFORCED HIGH DENSITY POLYETHYLENE

by

YOLANDA LEIGH HINTON

S.B.M.E., M.I.T.
(1977)

SUBMITTED IN PARTIAL FULFILLMENT
OF THE REQUIREMENTS FOR THE
DEGREE OF

MASTER OF SCIENCE
IN
MECHANICAL ENGINEERING

at the

MASSACHUSETTS INSTITUTE OF TECHNOLOGY

June 1980

Signature of Author _____
Department of Mechanical Engineering

Certified by _____
Bruce M. Kramer
Thesis Supervisor

Accepted by _____
Warren G. Rohsenow
Chairman, Department Graduate Committee

BALLISTIC IMPACT RESISTANCE

OF

FIBER-REINFORCED HIGH DENSITY POLYETHYLENE

by

Yolanda Leigh Hinton

Submitted to the Department of Mechanical Engineering
on May 11, 1980 in partial fulfillment of the
requirements for the Degree of Master of Science in
Mechanical Engineering

ABSTRACT

A viscous silicone oil coating was applied to glass and Kevlar fibers in a high-density polyethylene matrix. The composites were tested in ballistic impact, and the energy absorption measured as the loss in translational kinetic energy of a .22 caliber long rifle bullet with a muzzle velocity of 380 m/sec. Composites with coated 3-ply glass yarn absorbed 75.81 J, compared with 26.05 J absorbed by composites with uncoated glass yarn, an increase of 175%. Composites with triple strand untwisted glass fibers, and with Kevlar 29 and 49 fibers showed lesser increases in energy absorption with coated fibers. It is suggested with composites incorporating fibers with greater elongations-to-break show greater increases in energy absorption with coating on the fibers because of increased shear of the fluid coating, and that twisted fibers allow even more fluid shear as they elongate and untwist. Composites with coated fibers are proposed for high-velocity impact applications in automobiles and aircraft.

Thesis Supervisor: Bruce M. Kramer

Title: Assistant Professor
of Mechanical Engineering

for Danielle

For now we see through a glass, darkly; but then face to face: now I know in part; but then shall I know even as also I am known.

I Corinthians 13:12

ACKNOWLEDGEMENTS

The author wishes to acknowledge the assistance and support of all those who contributed to the effort involved in this thesis.

The academic support of Professors Nam P. Suh, Nak-Ho Sung and Bruce M. Kramer was much appreciated. The guidance provided by Mr. H. Dan Smith of Goodyear Aerospace Corporation was very welcome. For assistance in the shop and lab, thanks are due to the Technicians and Technical Instructors, Fred Anderson, Ralph Whittemore, Bob Kane, Fred Cote and John Ford. They were always available to assist with this work, teach proper methods and tolerate the mistakes and inconsiderateness of the author. The assistance of the members and students in the P^3 program was invaluable. Ben Su, Ken Smith, Rich Okine and UROP student Jim Garcia was most helpful in the lab. Don Huang was particularly helpful with tensile tests; Ken Griffiths was very helpful with Charpy. The assistance of all of these people is most gratefully acknowledged.

Tests conducted in the Strobe Lab at M.I.T. were facilitated by Harold "Doc" Edgerton, Bill MacRoberts, Charlie Miller and Jean Mooney. They are a great group of people who were very friendly, helpful and encouraging. Of them, the author is most appreciative.

For financial and moral support during three years of graduate study the author is indebted to Dr. John B. Turner, Associate Dean of the Graduate School, and to Professor H.H.

Richardson, Head of the Department of Mechanical Engineering. Jeanne Richard and Sandy Williams provided moral support and direction when it was most needed. To them the author extends a heartfelt thanks.

The author wishes to express her sincerest gratitude and appreciation to all her family and friends who provided moral and prayer support and inspiration. Myra Rodrigues merits special mention for being available to talk, counsel and provide direction to ease a life overcrowded and overwhelmed with school, family, friends and too many other activities. She was especially resourceful in helping to meet the needs of the author as a single parent of a beautiful, young lady. Also deserving of special mention is James E. Clark, a very special friend and confidant of the author. When problems and frustrations reached their summit, and hope, perseverance and determination faded almost completely away, he was available with a shoulder on which to cry and the words to motivate the author to carry on. To him, the author shall be eternally grateful.

Special thanks are due to Ms. Lisa Gibson for tolerating the author's procrastination and typing this document on such short notice. Her effort is much appreciated.

This work was supported by M.I.T., Ford Motor Co., and the MIT-Polymer Processing Program. The sponsors of P^3 have included the National Science Foundation, AMP, Inc., General Motors Corp., Gleason Works, Goodyear Tire and Rubber Co., Instrumentation Laboratory, Inc., International Telephone and

Telegraph Corp., Kendall Co., Eastman Kodak Co., Lord Corp., USM Corp., and Xerox Co.

TABLE OF CONTENTS

LIST OF FIGURES

LIST OF SYMBOLS

W_s = static work of plastic deformation of a plate perforated by a projectile

W_d = dynamic work of plastic deformation

σ_y = yield strength of a plate in uniaxial tension

ε_0 = maximum strain of plate in uniaxial tension

S = circumference of deformed area of plate

R = projectile radius

h_0 = plate thickness

r = radius of hole in perforated plate

m^* = displaced mass of perforated plate

t_0 = time for projectile to perforate plate

v_1 = initial projectile velocity

L = length of nose of projectile

P = density of plate

m = mass of projectile

ζ_x = momentum of plate within deformed region when perforated

ξ = deformation function

α = ½ nose angle of projectile

W_p = work of plastic deformation (static)

τ = shear strength of composite

γ = shear strain in composite

V = deformed volume of composite

σ_L = yield strength of composite

σ_f = tensile strength of fiber

V_f = fiber volume fraction

σ_m = stress in matrix when fiber breaks

W_b = work of plastic deformation of bullet

σ_b = yield strength of bullet

ε_b = strain in bullet

V_b = deformed volume of bullet

τ = shear stress in fiber

μ = viscosity of coating fluid

$\frac{dV}{dR}$ = shear strain rate of fluid

W_s = work of fluid shear

A = fiber surface area

r = fiber radius

ℓ = fiber length

V = initial bullet velocity

τ = coating thickness

W_f = energy absorbed in friction

f = coefficient of friction between fiber and matrix

I. INTRODUCTION

Fiber-reinforced thermoplastics are high strength materials which are easily processible into finished parts by thermoforming techniques. Increasing their energy absorption upon impact would make them attractive for high velocity impact applications such as automobile bumpers, highway guard rails, and aircraft and automobile fuel tanks.

Incorporation of high strength, high modulus fibers into thermoplastics generates significant increases in static properties including modulus of elasticity, tensile strength, and fracture strength, but tends to decrease the impact resistance of the material. The effect of the fibers is to initiate and propogate cracks, and to cause localized stress concentrations that lead to brittle fracture in materials which would otherwise yield under impact loading without catastrophic failure.

The methods of energy absorption operative upon failure of a fiber-reinforced plastic include fracture of the composite, fiber-matrix debonding, and fiber pullout from the matrix. The fracture energy of a given fiber-matrix system can be increased with fillers and carefully controlled processing, but the improvements possible with these techniques are very limited. Previous attempts at increasing energy absorption have concentrated on fiber-matrix debonding and fiber pullout.

1.1 Previous Attempts at Increasing Energy Absorption

Atkins and Martson[1] experimented with alternating regions of strong and weak fiber-matrix interfacial bonding within composite materials. Regions of weak bonding were produced by coating the fiber surface with silicone vacuum grease or polyurethane varnish. The strong bonds imparted static strength to the matrix material, while the weakly bonded areas served to blunt the tips of propagating cracks, thereby increasing fracture toughness.

Morley, et al.[2] incorporated a duplex fiber consisting of an outer core strongly bonded to the matrix, and an inner core weakly bonded to the outer core. The composites supported static loads greater than those supported by conventional materials, absorbed large amounts of energy in cyclic loading, and absorbed up to 2.5 times as much energy as austenitic stainless steel in ballistic impact.

Favre[3] used various materials as delamination promoters between layers of graphite fibers, graphite-epoxy prepregs or graphite-phenolic prepregs and epoxy-resin. He found an increase in energy absorption in composites which normally display brittle modes of fracture when as little as a three percent volume fraction of thin metallic or polymeric sheets was incorporated into the lay-up, with no effect on static and fatigue strength. The method proved inadequate, however, for composites where pullout, debonding or delamination mechanisms were already predominant in fracture.

Jones[4] presented the concept of coating the fibers with a viscous fluid to increase the fracture toughness of composites. By optimizing coating thickness such that the shear force in the fluid coating is maximized without exceeding the tensile strength of the fiber, a large amount of energy can be absorbed in the fluid as the fiber is pulled from the matrix. For a composite of glass fibers coated with silicone oil in a brittle polyester matrix, Jones increased fracture toughness as measured by Izod tests by more than 150% over that of uncoated glass fiber-polyester composites. The potential applicability of the process to a polyethylene matrix was demonstrated by a ballistic impact test in which energy absorption of a coated fiber composite increased by 11% over that of an uncoated fiber composite.

1.2 Impact Testing of Fiber-Reinforced Thermoplastics

Thermoplastic materials are very ductile at low strain rates and tend to not break in conventional Izod and Charpy impact tests. Jones[5] demonstrated that glass-HDPE composites could be perforated by a 17-grain pellet at velocities exceeding 779.2 ft/sec (256 m/sec).

Impact tests providing complete breakage or perforation of the samples were desirable, as is a complete break in conventional tests, for comparison of energy absorption among different composites. With the expectation of increasing energy absorption and, therefore, perforation velocity, a high velocity ballistic impact test was selected.

1.3 Studies of Ballistic Impact

1.3.1 Energy and Momentum Analysis. Goldsmith[6] analyzes projectile penetration and perforation of thin plates from both energy and momentum considerations. His energy analysis considers a static work term of plastic deformation, and a dynamic work term associated with accelerating the deformed portion of the plate from rest to the speed of the projectile assuming the plate deforms to the geometry of the projectile. These are given respectively as:

$$W_s = \sigma_y \int d\varepsilon_0 = \sigma_y \int_0^r \frac{ds}{s}$$

or

$$W_s = \tfrac{1}{2} \pi R^2 h_0 \sigma_y$$

and

$$W_d = \int F \cdot dr = \int_0^t m^* \frac{d^2r}{dt^2} dr + \int_0^{t_0} \frac{dm}{dt} \frac{dr}{dt} dr$$

where

σ_r = yield stress of plate in uniaxial tension

h_0 = plate thickness

R = projectile radius

r = radius of hole in plate

m^* = displaced mass

t_0 = time for projectile to perforate plate

and r is a function of time.

The dynamic work integral can be calculated for a given projectile geometry. For an ogive, the standard ammunition geometry.

$$r = R \sin \frac{\pi}{2} \frac{v_1 t}{L}$$

where

v_1 = initial projectile velocity

L = length of nose of projectile

assuming constant velocity during perforation. Equation 2 then gives

$$W_d = 1.86\rho \left(\frac{v_1 R}{L}\right)^2 \Pi h_0 R^2$$

ρ = density of plate

Combining W_s and W_d we get total work for a thin plate perforated (completely penetrated) by an ogival projectile as:

$$W = \Pi h_0 R^2 \left[1.86\rho \left(\frac{v_1 R}{L}\right)^2 + \tfrac{1}{2} \sigma_y\right]$$

Goldsmith's momentum analysis considers the initial momentum of the projectile, mv_1, to be equal to the sum of the final projectile momentum mv and ζ_x, the plate momentum within the deformed region, when ζ_x is given as:

$$\zeta_x = 2 \Pi \rho h_0 \int_0^r v r_0 \frac{\partial \xi \langle r_0, x \rangle}{\partial x} dr_0$$

The function $\xi \langle r_1, x \rangle$ is a deformation function postulated from experimental observation. In the case of a conical projectile of nose angle 2α, perforating a plate which deforms to its shape,

$$\xi = x (\tan\alpha - r_0) \cos\alpha$$

and

$$\zeta_x = \Pi \rho h_0 v \tan\alpha (1-\sin\alpha)(x\tan\alpha)^2$$

This analysis agrees well with experiments but postulates no relation between material properties and energy absorption.

1.3.2 Force-Velocity Analysis. Awerbuch and Bodner[7] consider a three-stage penetration during projectile perforation of metallic plates. In the first stage, inertial forces resist acceleration of the mass of the plate in contact with the projectile and compressive forces due to the compressive strength of the plate material act to resist the projectile. These forces continue to act during stage two penetration. In addition, a shear force results from relative motion between the plate and a plug of plate material which accelerates with the projectile. In the third stage the ejected plug moves with the projectile and is acted upon only by a shear force on its surface area. When accompanied with experimentally determined deformation geometries, this force analysis provided good predictions of post-perforation projectile velocities and perforation times. It provides no correlation, however, between material properties and these empirical considerations.

Energy absorption in perforation of fiber-reinforced thermoplastics is expected to be determined by plastic deformation and fracture of the composite, plastic deformation of the bullet, fiber elongation and fluid shear, and inertia and friction effects. Each of these energy absorbing mechanisms is considered below.

2.1 Plastic Deformation and Fracture

Assuming the composites to be rigid-perfectly plastic, the work of plastic deformation, W_p, is given by

$$W_p = \int \tau \gamma \, dV$$

where

τ = shear strength of composite

γ = shear strain in composite

V = deformed volume of composite

Shear strength of the composite can be taken as one-half the tensile strength by the von Mises' yield criterion. Tensile strength is given by

$$\sigma_c = \sigma_f V_f + \sigma_m' (1-V_f) \qquad (2.1)$$

where

σ_c = composite strength

σ_f = fiber strength

V_f = fiber volume fraction

σ_m' = stress in matrix when fiber breaks

The stress in the matrix when the fibers break is either the matrix yield stress σ_y, or the product of matrix modulus and ultimate elongation of the fibers $E_m \varepsilon_f$, whichever is less.

W_p, then, is given by

$$W_p = \int \tfrac{1}{2} \left[\sigma_f V_f + \sigma_m' (1-V_f)\right] \gamma \, dV \qquad (2.2)$$

where shear strain, γ, and deformed volume, V, are measured from tested samples.

2.2 Bullet Deformation

The work of plastic deformation of the bullet is likewise.

$$W_B = \int \sigma_b \varepsilon_b \, dV_b \qquad (2.3)$$

where

σ_b = bullet yield strength

ε_b = strain in bullet

V_b = deformed volume of bullet

The yield strength for lead can be found in tables; the strain and deformation are measured from the test samples.

2.3 Fiber Elongation and Fluid Shear

Fiber motion relative to the matrix, whether by elongation or pullout, causes shear in the fluid coating the fiber. For viscous Newtonian fluids, the shear stress resisting fiber motion is

$$\tau = \mu \frac{dV}{dR}$$

and the energy absorbed in shear is

$$W_s = \int \tau \, dA \, ds$$

where

τ = shear stress on the fiber

μ = fluid viscosity

$\frac{dV}{dR}$ = strain rate

A = fiber surface area = $2\Pi r \ell$

ds = change in fiber length

Assuming the fiber moves with the bullet at velocity V, within a uniform coating of thickness t, the strain rate in the fluid may be estimated as V/t. If the fiber elongates to its breaking strain, ds can be estimated as $\ell d\varepsilon$ where ℓ is the length of fiber elongated as measured from the deformed area in the tested samples, and $d\varepsilon$ is the ultimate fiber elongation. Energy absorption is then given as:

$$W_s = \int \mu \frac{V}{t} 2 \pi r \ell^2 \, d\varepsilon \qquad (2.4)$$

2.4 Inertia and Friction Terms

An inertia or dynamic work term may be evaluated as proposed by Goldsmith.[8] Assuming the deformed volume dV of the composite to be accelerated from rest to the bullet velocity, the energy required is

$$W_d = \int m \frac{dr^2}{dt^2} dr + \int \frac{dm}{dt} \frac{dr}{dt} dr$$

where

m = displaced mass

r = radius of determined area

For a standard bullet of ogival geometry

$$r = R\sin\frac{\pi}{2}\frac{Vt}{L}$$

where

R = bullet radius

V = bullet velocity

t = time required for bullet to perforate plate

L = length of bullet nose

Evaluating the integral for W_d gives

$$W_d = 1.86\rho\left(\frac{VR}{L}\right)^2 \pi h_0 R^2 \qquad (2.5)$$

where

ρ = density of plate

h_0 = thickness of plate

A frictional energy term can be estimated assuming a normal force equal to the yield stress of the matrix acts over the surface area of the bullet. This gives

$$W_f = f\sigma_y A = f\sigma_y (2\pi r\ell) \qquad (2.6)$$

where

f = friction coefficient

σ_y = matrix yield stress

A = fiber surface area

2.5 Summary

The energy absorbed in fiber pullout or elongation, and fluid shear is dependent upon fluid viscosity, strain rate, coating thickness and fiber properties. Varying the thickness of the fluid coating on the fiber will vary the strain rate in

the fluid. The viscosity of the fluid will also vary, as a result of its strain rate dependence as shown in Figure 2.1. At exceedingly high strain rates, applied for short time spans, the fluid displays a transient response as shown in Figure 2.2. Increasing coating thickness will decrease strain rate, and, if viscosity effects are predominant, will decrease energy absorption. If, however, the strain rate is high enough and duration of the deformation is short enough that transient response is the major effect, energy absorption should follow a curve similar to the transient response of the fluid. Expectations are that the transient response will predominate at small coating thicknesses, and strain rate-viscosity effects will predominate at greater coating thicknesses.

Energy absorption in fluid shear is also dependent upon the behavior of the fiber. A strong fiber may withstand the impact of a bullet and be pulled from the matrix, causing fluid shear along the entire length of the fiber. A weaker fiber would break, absorbing only the energy required to break it. A fiber strong enough not to break immediately upon impact, yet not strong enough to be pulled from the matrix, should elongate before breaking, causing fluid shear and energy absorption along the portion which elongates. A more elastic fiber should, therefore, lead to more energy absorption.

The energy absorbed in deforming and fracturing the composite is a strong function of composite strength, assuming the composite will fracture in a brittle manner at ballistic impact velocities. Since composite strength is directly

THE ORIGINAL PRINT ON THE FOLLOWING PAGES IS ILLEGIBLE

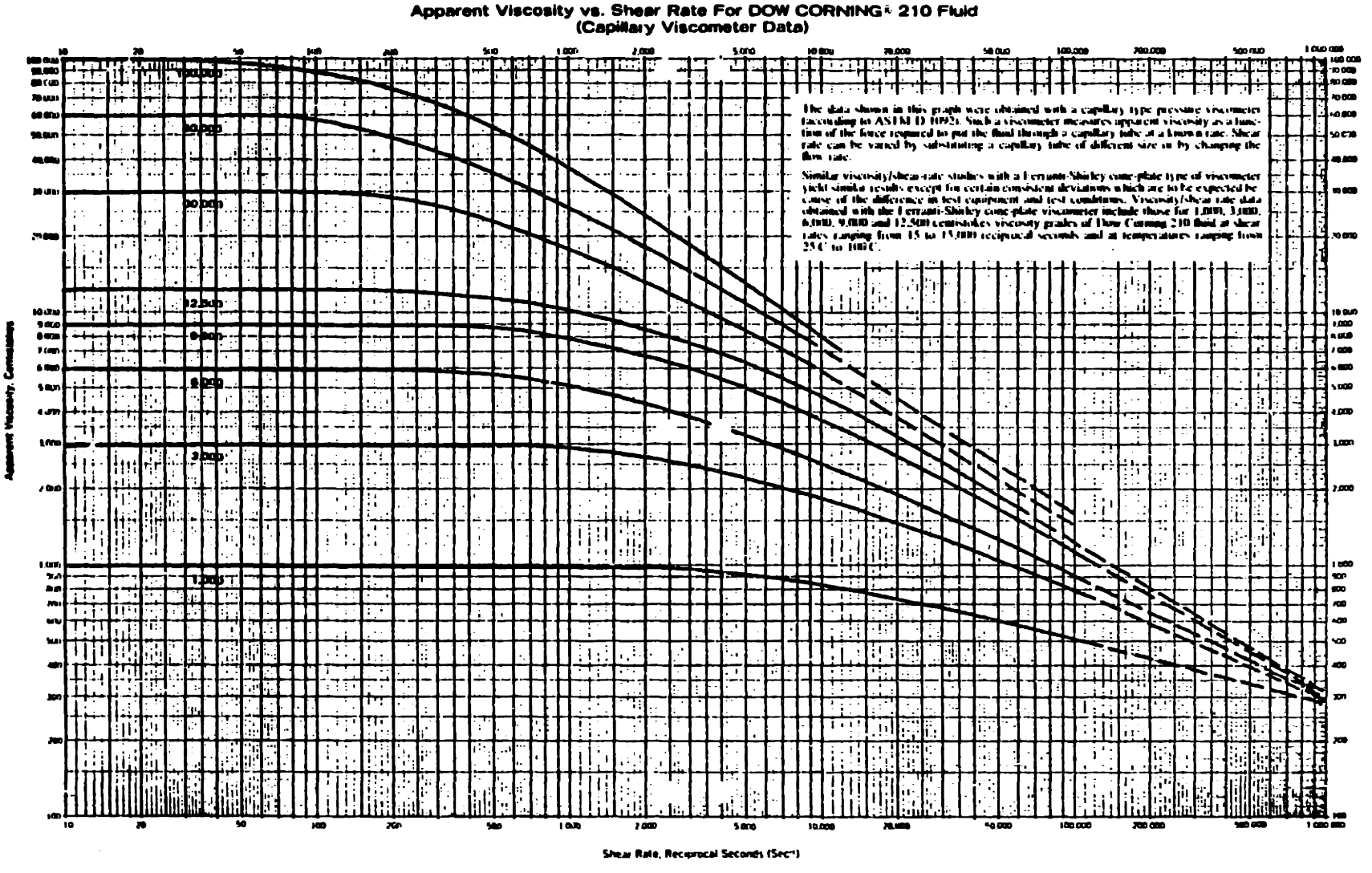

FIGURE 2.1: VISCOSITY-STRAIN RATE RELATION OF DOW CORNING 200 AND 210 FLUIDS[9]

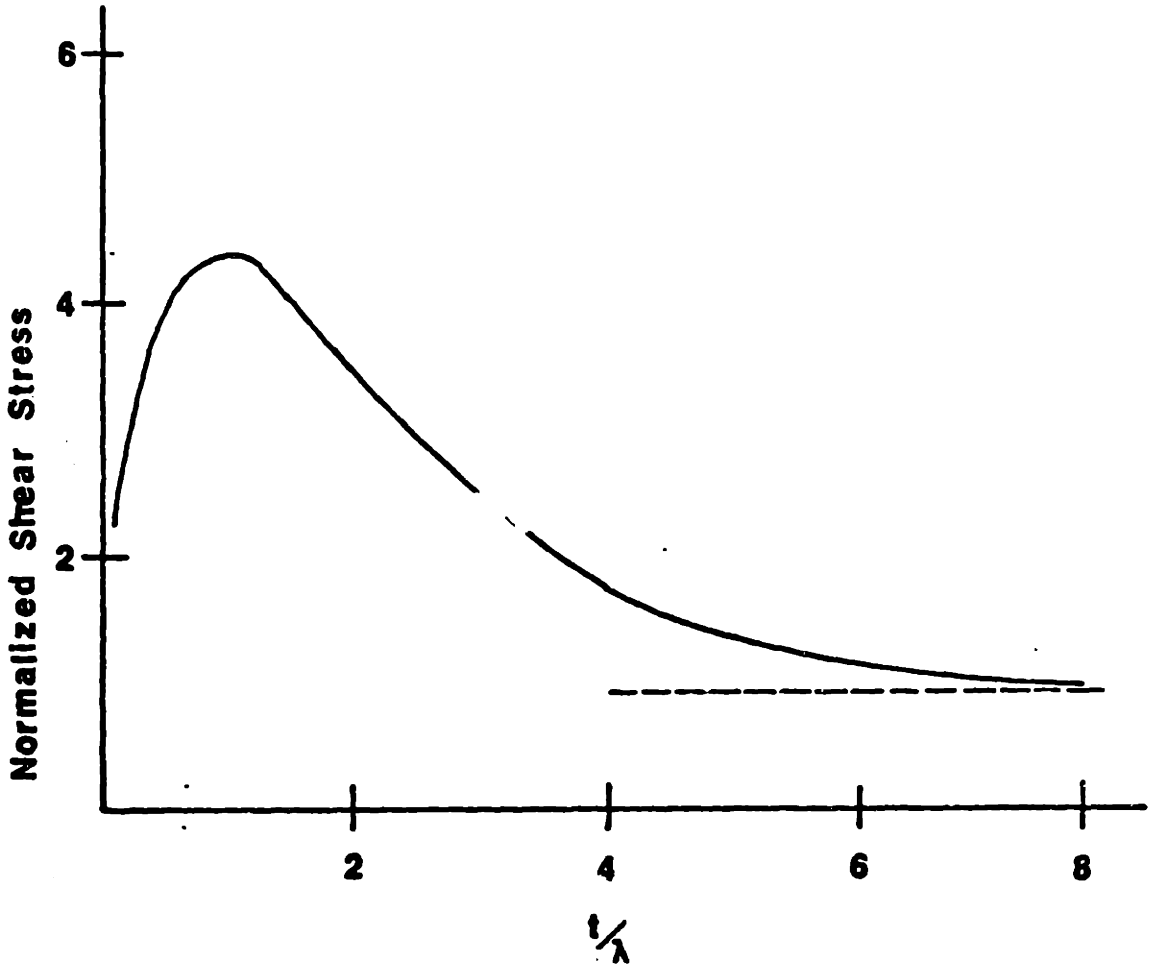

FIGURE 2.2: TRANSIENT SHEAR STRESS OF VISCOELASTIC FLUID[10]

related to fiber strength by Equation 2.2, a stronger fiber should increase energy absorption. This increase is expected to be not as pronounced as the increase in energy absorption with coating thickness and fiber elasticity.

Energy absorption associated with bullet deformation and inertia effects is not expected to vary very much with changes in coating thickness or fiber properties. No energy is absorbed in friction between fiber and matrix when the fibers are coated. Experiments to substantiate the theoretical analysis contained herein are described in the next chapter.

III. EXPERIMENTAL PROCEDURES

A program utilizing Jones' method of toughening composites with a viscous fluid coating on the fibers, and using ballistic impact tests to determine energy absorption was conducted. Thermoplastics were selected as the matrix material because of their ductility and high fracture toughness.

3.1 Materials

3.1.1 Matrix. A Texaco high-density polyethylene was used as the matrix material. It's ability to flow at low temperature (125^{o}C), to mold without leaving apparent voids, and to cool without crystallizing contributed to the ease of fabricating composites. Its properties are shown in Table 3.1.

3.1.2 Fluid Coating. DC-200, a Dow-Corning polydimethylsiloxane fluid, was used to coat the fibers. Because the energy absorbing capability of the composite is expected to increase with the viscosity of the fluid, the highest available viscosity fluid, 100,000 centistokes, was used.

3.1.3 Fibers. Composites were made with both glass and Kevlar fibers. Owens-Corning Fiberglas ECG 75 1/0, a one-ply glass yarn with Z 30 TPM (i.e., 30 twists per meter in a "Z" configuration, 0.7Z twists per inch), were used in a single strand configuration, as well as a triple strand configuration with no further twisting. Owens-Corning ECG 75

TABLE 3.1: PROPERTIES OF HDPE

Yield Strength	3×10^7 N/m^2
Elongation at Yield	9%
Ultimate Tensile Strength	3×10^7 N/m^2
Ultimate Elongation	600%
Modulus of Elasticity	1×10^9 N/m^2
Flexural Strength	4.9×10^7 N/m^2
Flexural Modulus	1.5×10^9 N/m^2
Compressive Strength	4.5×10^7
Poisson's Ratio	0.43
Bulk Modulus	5.0×10^9 N/m^2
Density	0.97×10^3 kg/m^3
Melting Temperature	125° C

1/3, a 3-ply yarn with Z 163TPM (3.8Z TPI) was used as supplied. Composites were also made with DuPont Kevlar 49 and 29 single strand fibers with no twist; both are high strength fibers of an aromatic polyamide. Kevlar 29 was also plied and twisted into a 3-ply yarn to compare with the 3-ply glass yarn composites. The physical and mechanical properties of the fibers are shown in Table 3.2.

3.2 Fabrication

Composites were made by passing continuous strands of fiber through a beaker of silicone oil, and through one or more dies of varying diameters to control coating thickness. The fibers were wrapped around a 12" square by 1/8" thick aluminum frame which was mounted in an engine lathe. The fibers were fed along the length of the frame by the lathe tool bed as the frame rotated in the chuck, such that they were evenly spaced along the frame. Layers of 15 mil (.006 cm) HDPE film were alternated with layers of fibers. The frame was rotated 90^{o} after each layer of fiber was layed-up, resulting in a biaxial fiber orientation. For the initial glass and Kevlar composites, fiber spacing was 28 per inch (11.28 per cm); the triple strand glass fibers were spaced 14 per inch (5.6 per cm). After lay-up on the lathe, the entire assembly of 12 layers of fibers and 15 layers of HDPE was placed in a hot press with 9-inch square aluminum face plates, heated to 130^{o}C, and molded under 65 psi pressure for 30 minutes. The

TABLE 3.2: PROPERTIES OF GLASS AND KEVLAR FIBERS

	3-ply Glass	1-ply Glass	Kevlar 29	Kevlar 49
Tensile Strength (NM/m^2)	690	690	2758	2758
Modulus of Elasticity (MN/m^2)	72000	72000	62000	124110
Elongation to Break	4.8%	4.8%	4.0%	2.5%
Density (g/cm^3)	2.54	2.54	1.44	1.44
Denier	1786	595	200	195
Diameter (cm)	.007	.004	.002	.002

composites were left in the press to cool, and then cut into 4 inch (10 cm) square panels, approximately ¼ inch (0.6 cm) thick. One hundred foot lengths of the fibers were weighed before and after coating to determine the amount of fluid coating on the fibers. It is given in weight of fluid per unit length of fiber. Figures 3.1 and 3.2 show fabrication of the composites and the finished composite.

3.3 Test Procedures

3.3.1 Tensile Tests. Each of the fibers was tested in tension in an Instron machine to measure fiber strength, elongation and modulus of elasticity. Samples were prepared by placing fibers between cardboard tabs, securing them with epoxy cement, and cushioning them with RTV Silicone Rubber to prevent breakage at the edges of the cardboard tabs. One of the Tensile Test specimens is shown in Figure 3.3. The samples were clamped in the machine and tested at a crosshead speed of 0.5 inches per minute, with an 8-inch gage length between the clamps.

3.3.2 Ballistic Tests. Ballistics tests were conducted in the Strobe Laboratory at MIT. The composites were held in a clamp and fired at with a .22 caliber long rifle, using 40 grain bullets with a muzzle velocity of 380 m/sec (1160 ft/sec). An EG&G Mutliple Microflash Unit was triggered by a microphone pickup of the sound of the rifle to flash a strobe light 10 consecutive times at 100 μsec intervals (10

FIGURE 3.1: FABRICATION OF COMPOSITES

FIGURE 3.1: FABRICATION OF COMPOSITES

FIGURE 3.1: FABRICATION OF COMPOSITES

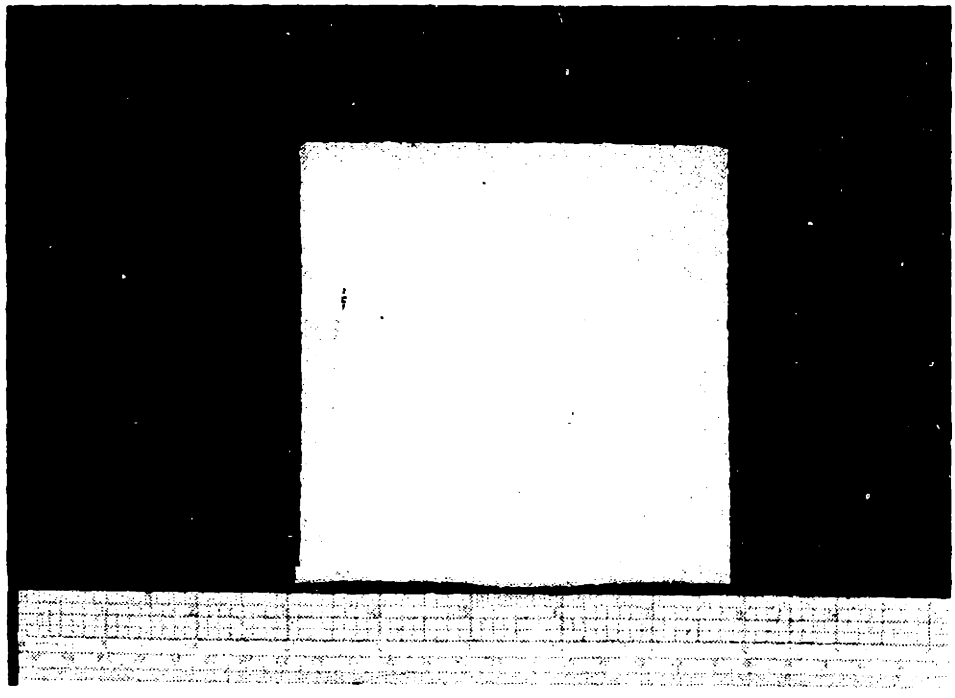

FIGURE 3 2: FINISHED COMPOSITE

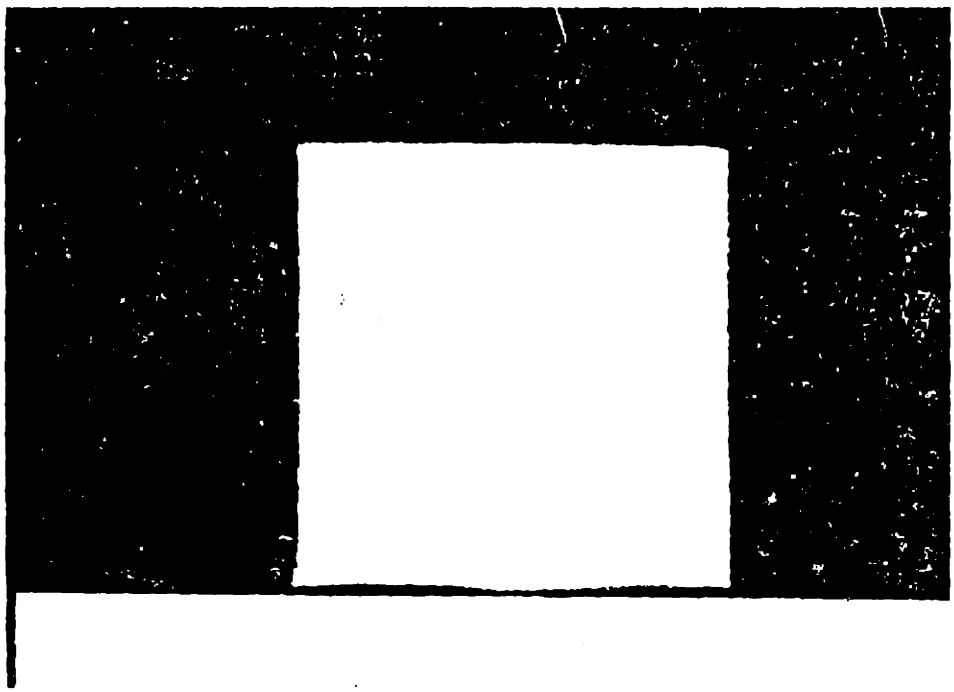

FIGURE 3 2: FINISHED COMPOSITE

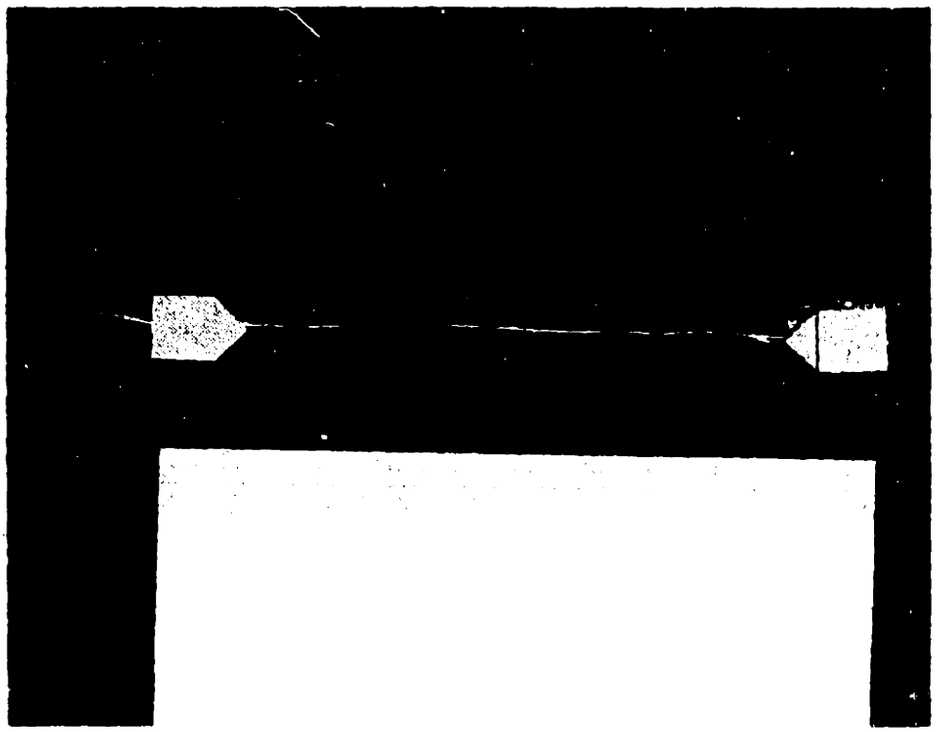

FIGURE 3.3: TENSILE TEST SPECIMEN

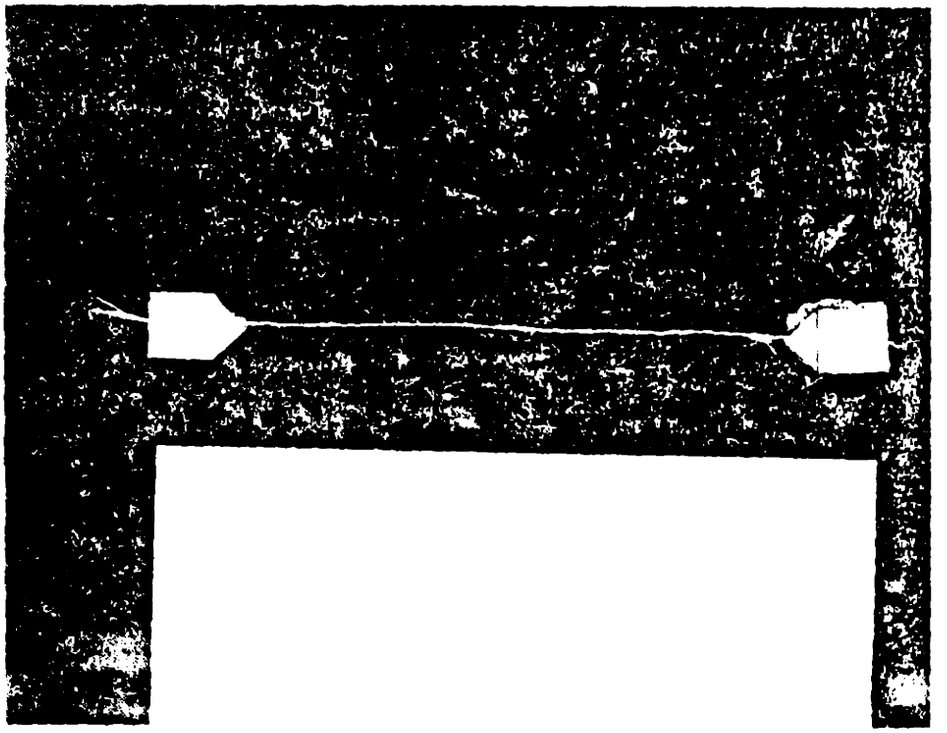

FIGURE 3.3: TENSILE TEST SPECIMEN

KHz frequency). A camera with open shutter in a darkened room recorded the event on Polaroid film. The resulting photograph showed ten consecutive images of the bullet and sample, before, during and after perforation, from which was measured the initial and final bullet velocities. The energy absorbed by the composite was calculated as the change in the translational kinetic energy of the bullet. The test set-up and one of the resulting photographs are shown in Figures 3.4 and 3.5 respectively.

3.3.3 Charpy Tests. Some of the samples were tested in a Tinius & Olsen Charpy Impact tester to compare energy absorption at a lower impact velocity than that of ballistic tests. Samples were cut from the prepared panels at one inch (2.5 cm) widths, approximately ¼ inch (0.6 cm) thick and 4 inches (10 cm) long.

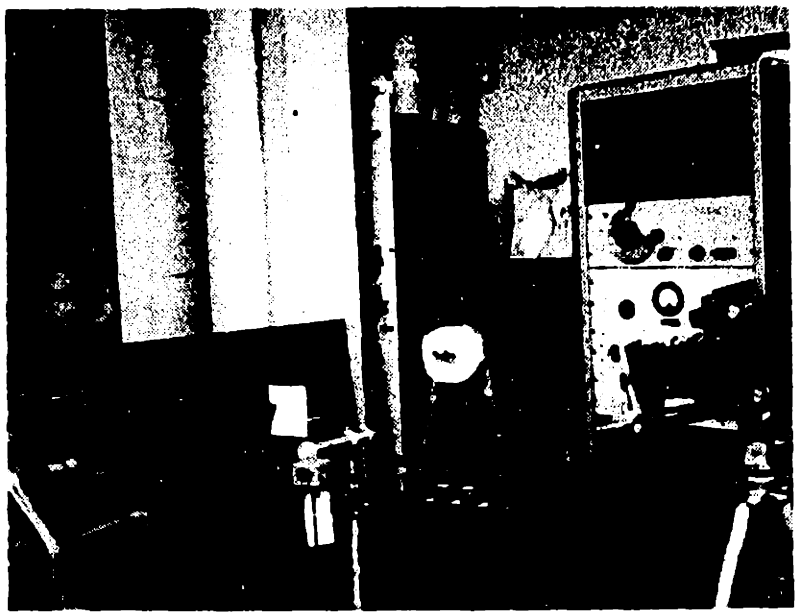

FIGURE 3.4: BALLISTICS TEST SET UP

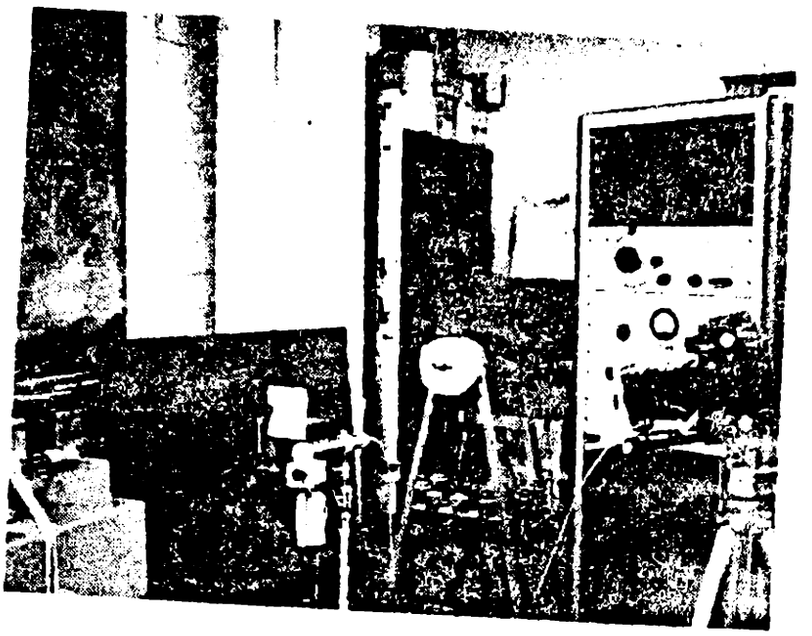

FIGURE 3.4: BALLISTICS TEST SET UP

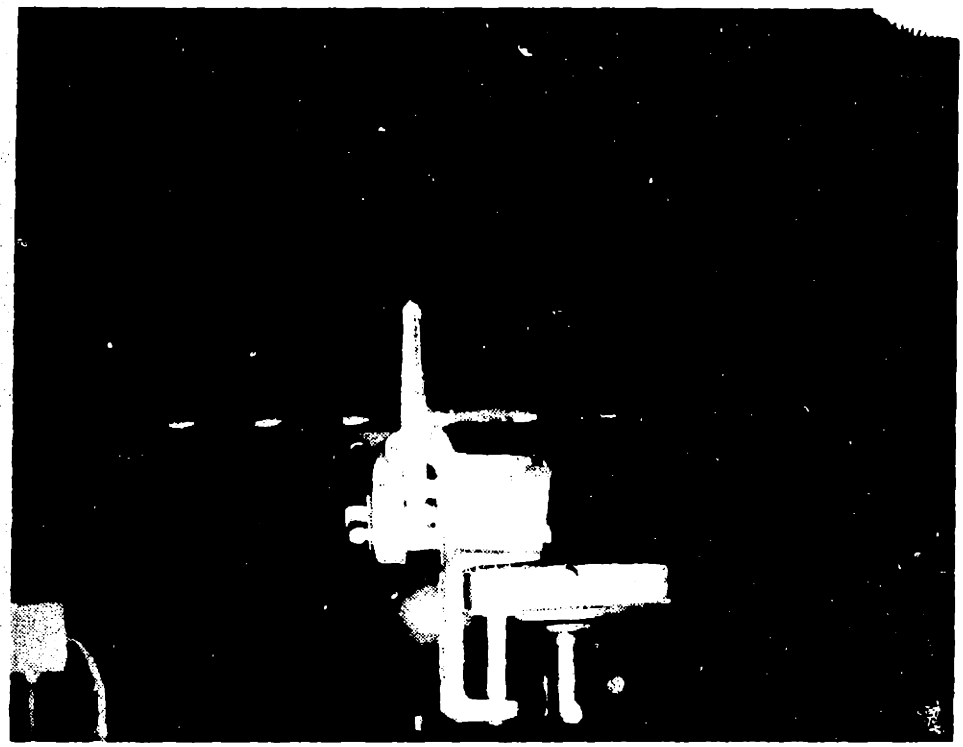

FIGURE 3.5: MULTIPLE MICROFLASH PHOTOGRAPH OF BALLISTIC IMPACT

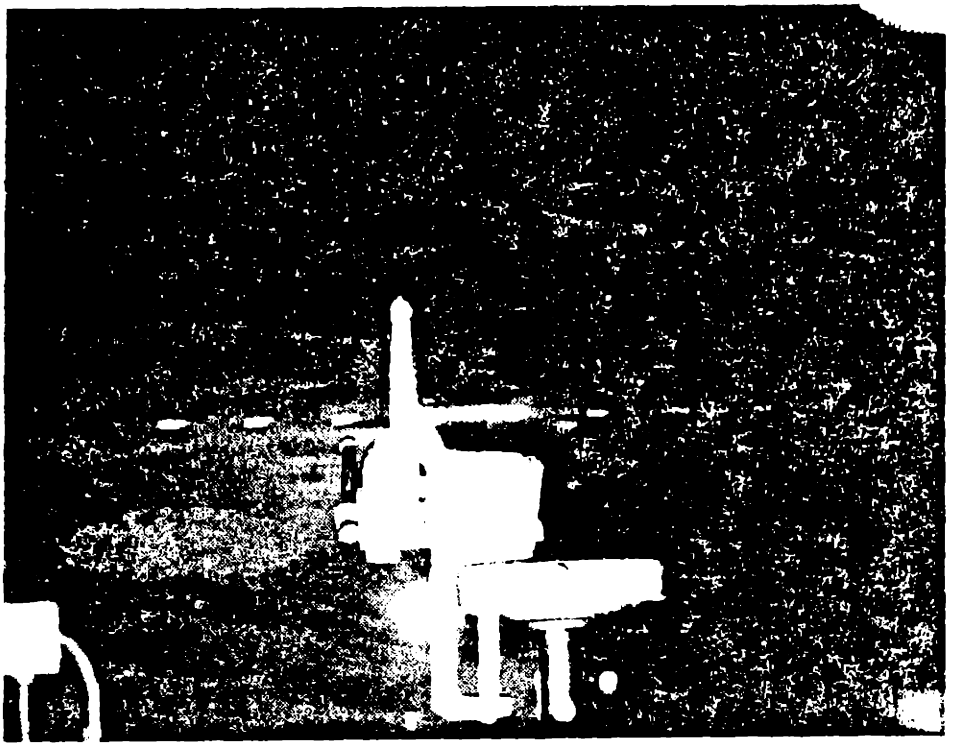

FIGURE 3.5: MULTIPLE MICROFLASH PHOTOGRAPH OF BALLISTIC IMPACT

IV. RESULTS

4.1 Tensile Tests

The fiber properties measured in tensile tests are shown in Figure 4.1.

4.2 Ballistics Tests

4.2.1 Three-ply Glass Yarn. The energy absorption of composites with three-ply glass yarn is shown in Figure 4.2. The composites with zero coating on the fibers absorbed 23.73J. Energy absorption increased with amount of coating by 175%, to 75.81J at a fluid coating of 9.17×10^{-4}g/cm of fiber length, which corresponds to a coating thickness of 5.97×10^{-3}cm, with excessively heavy and non-uniform coatings, the energy absorption decreased.

4.2.2 Triple Strand Glass Fiber. Attempts to make composites with single strand glass fibers were unsuccessful because the small diameter of the fibers made them difficult to handle without abrasion and subsequent breakage, and difficult to evenly coat with the coating fluid. The strands were tripled to overcome these problems, and to compare with the three-ply twisted yarn. The fiber volume fraction was reduced to maintain spacing between fibers.

The control samples with triple strand glass fibers absorbed 30.67 J. Energy absorption increased by 50% to 46.01 J at a coating of 9.11×10^{-4}g/cm, or 8.45×10^{-3}cm.

	Tensile Strength	Elongation to Break	Modulus of Elasticity
3-ply Glass	63 x 10^3psi (434 MN/m^2)	1.95%	3.2 x 10^6psi (22064 MN/m^2)
Triple Strand Glass	52 x 10^3psi (359 MN/m^2)	2.06%	2.55 x 10^6psi (17582 MN/m^2)
Kevlar 49	103 x 10^3psi (710 MN/m^2)	1.95%	5.29 x 10^6psi (36475 MN/m^2)
Kevlar 29	194 x 10^3 (134 MN/m^2)	3.48%	5.57 x 10^6psi (38405 MN/m^2)

FIGURE 4.1: TENSILE TEST RESULTS

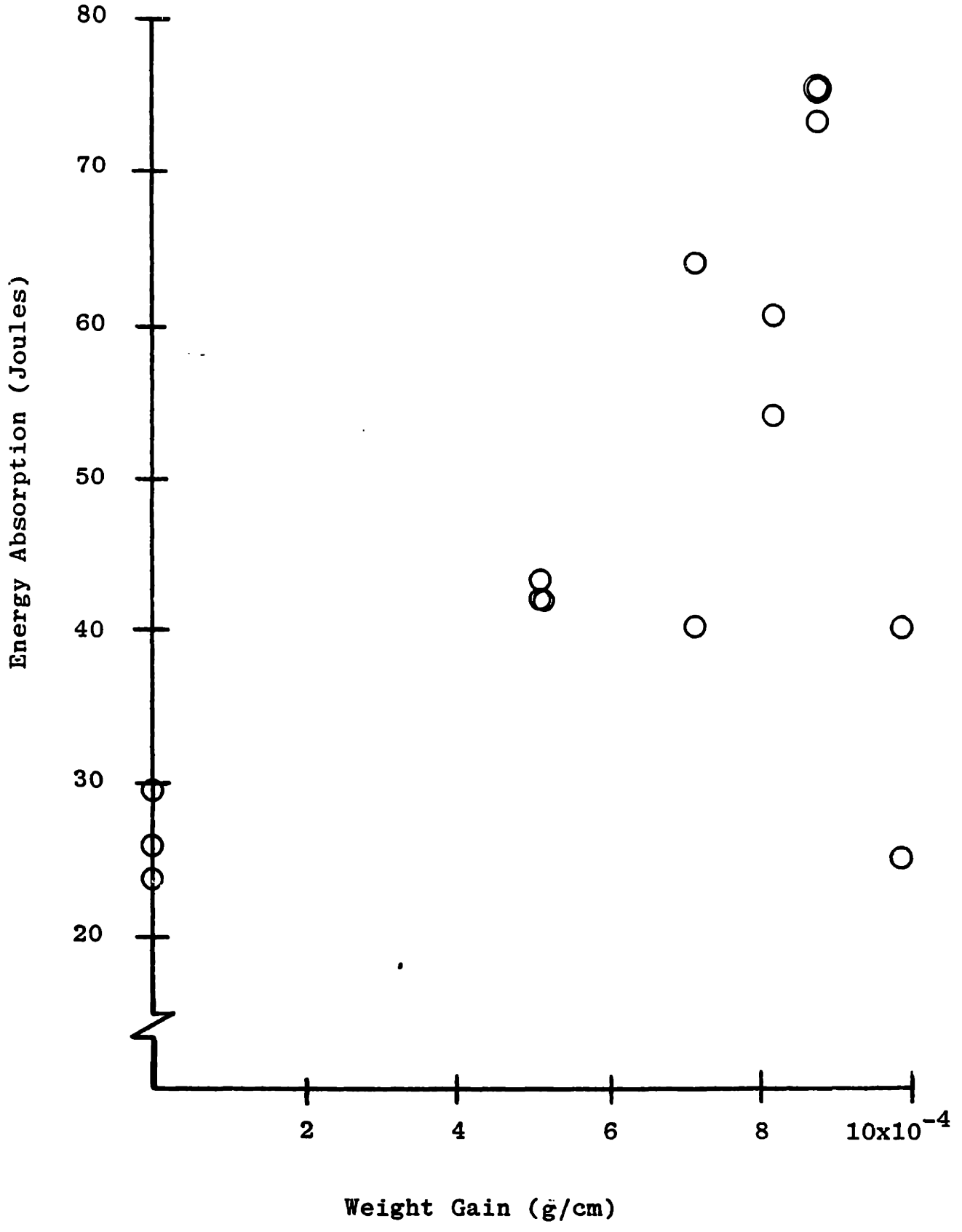

FIGURE 4.2: THREE-PLY GLASS YARN COMPOSITES - RESULTS

The results are shown in Figure 4.3.

4.2.3 Kevlar 49 Fibers. Kevlar 49 - HDPE composites absorbed 23.07 J with zero coating on the fibers. Energy absorption increased 57% to 36.29 J at a fluid coating of 3.4×10^{-4} g/cm, or 4.57×10^{-3} cm. The increase in energy absorption is less dramatic than that demonstrated by the glass yarn composites, and, as can be seen in Figure 4.4, is not as consistent with the amount of fluid coating on the fibers.

4.2.4 Kevlar 29 Fibers. The results of tests conducted on composites made with Kevlar 29 fibers are shown in Figure 4.5. The samples with uncoated fibers absorbed 24.62 J. Energy absorption increased by 65% to 40.53 J at a coating of 0.371×10^{-4} g/cm, or approximately 9.5×10^{-3} cm coating thickness. The increase in energy absorption is greater than that of the composites made with Kevlar 49, but less than the increase in energy absorption of composites made with 3-ply glass yarn.

Kevlar 29 fibers were plied and twisted into the same configuration as the 3-ply glass yarn for direct comparison with that yarn. The silicone oil, however, failed to wet the yarn.

4.3 Charpy Tests

The samples tested in Charpy impact tests failed to break. The impact strength of the materials could, therefore,

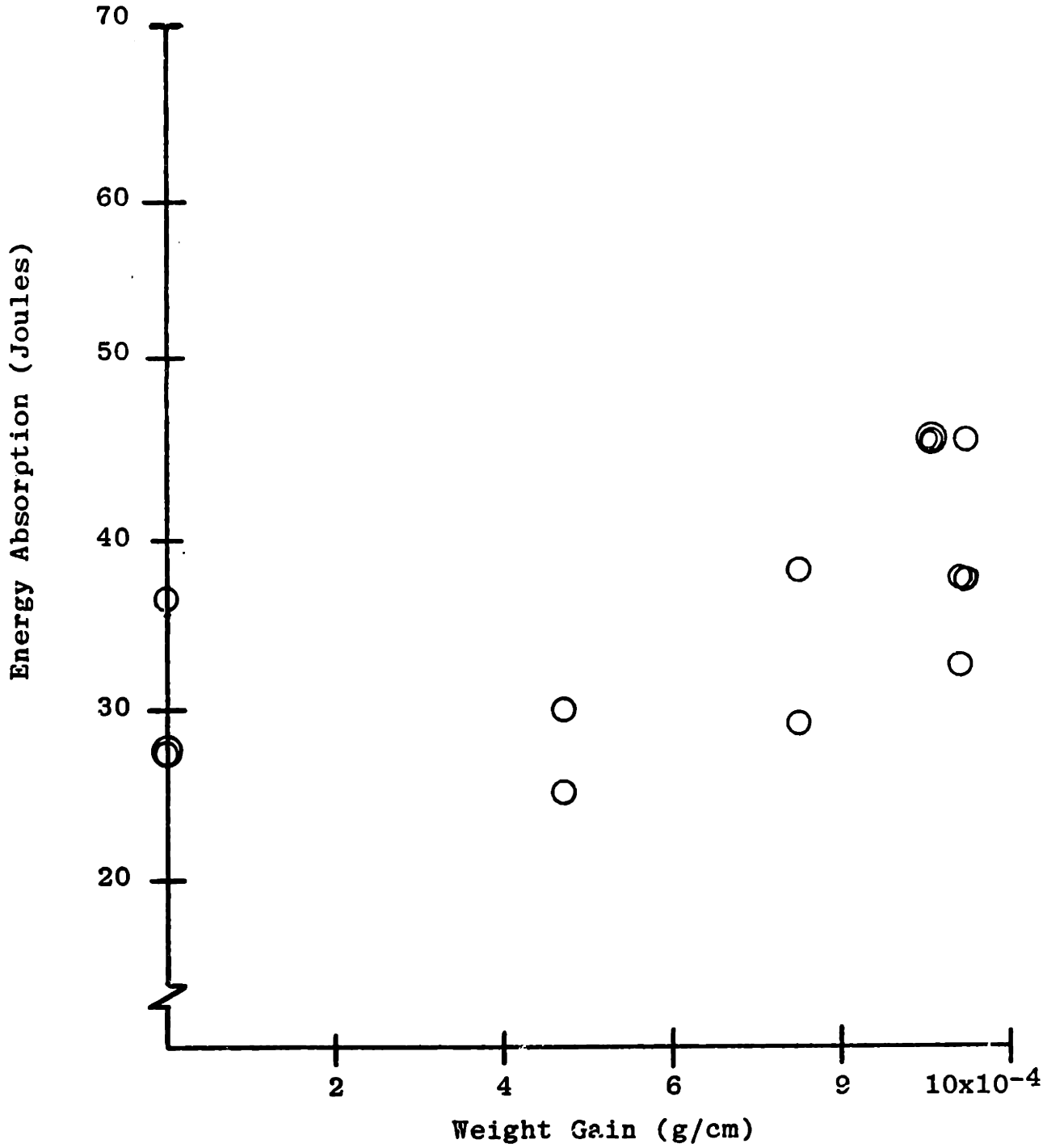

FIGURE 4.3: TRIPLE STRAND GLASS FIBER COMPOSITES - RESULTS

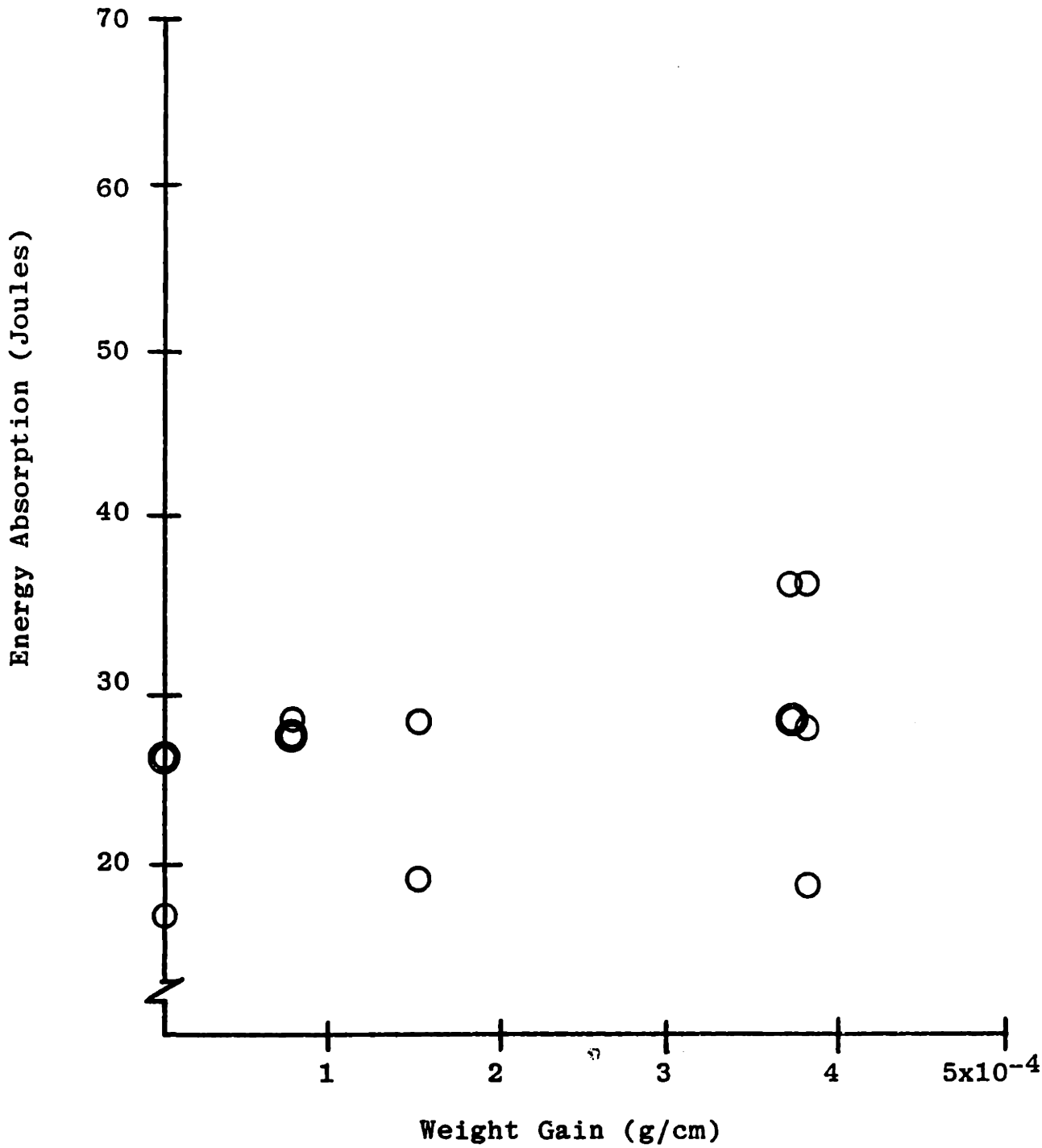

FIGURE 4.4: KEVLAR 49 FIBER COMPOSITES - RESULTS

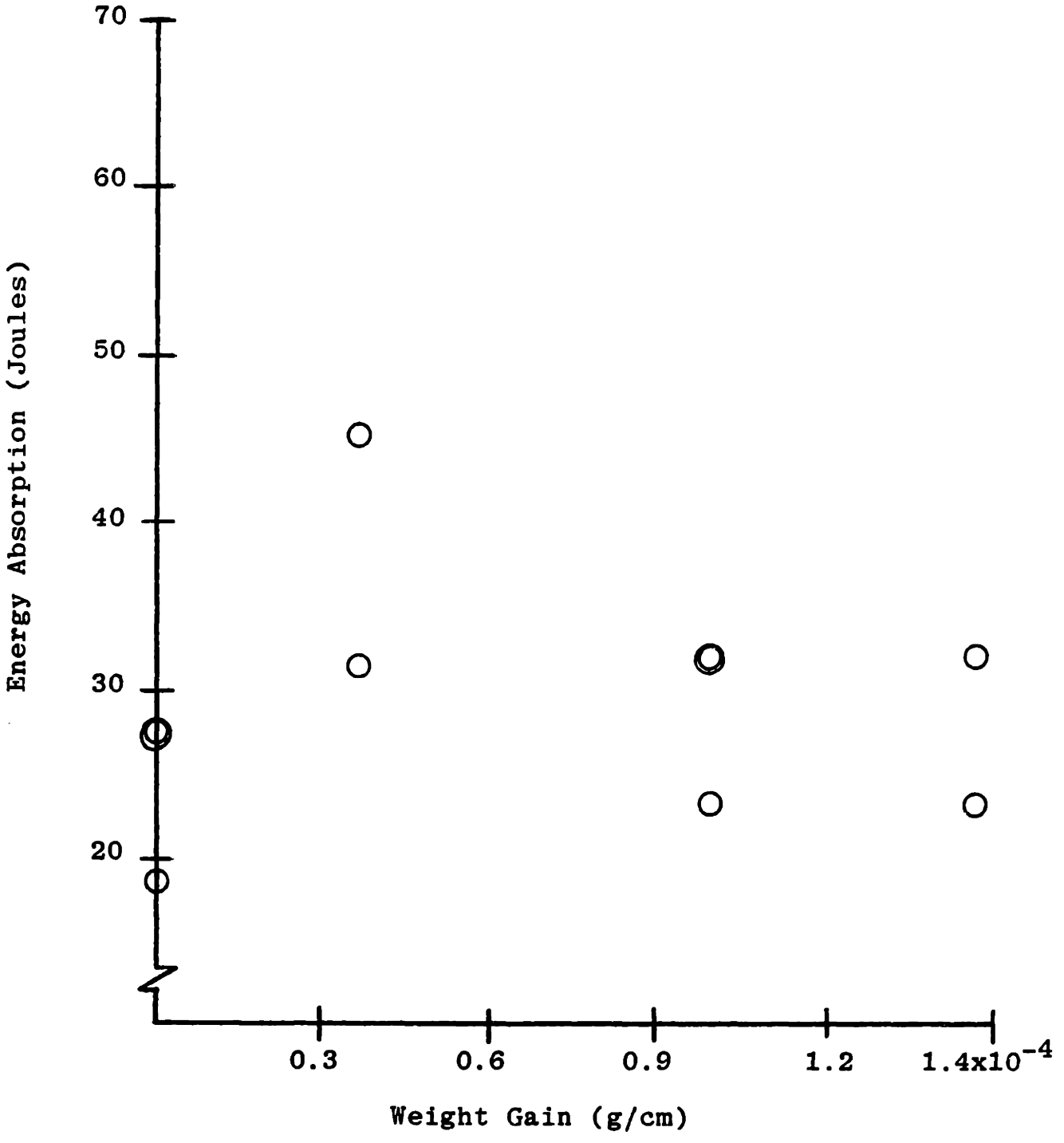

FIGURE 4.5: KEVLAR 29 FIBER COMPOSITES - RESULTS

not be measured. The samples, after impact, are shown in Figure 4.6.

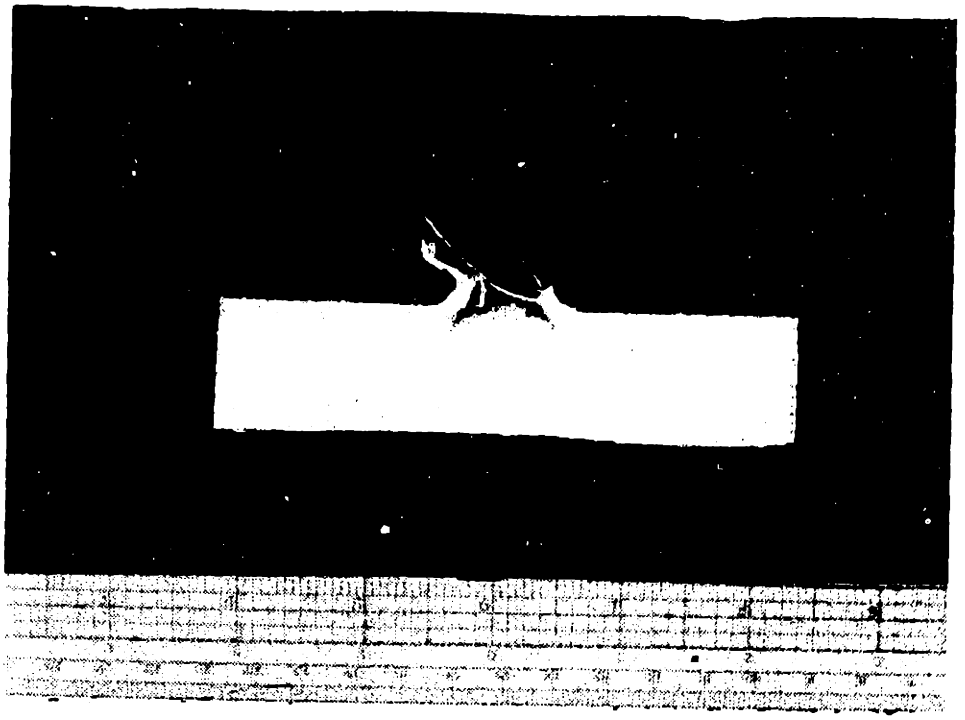

A. Unnotched

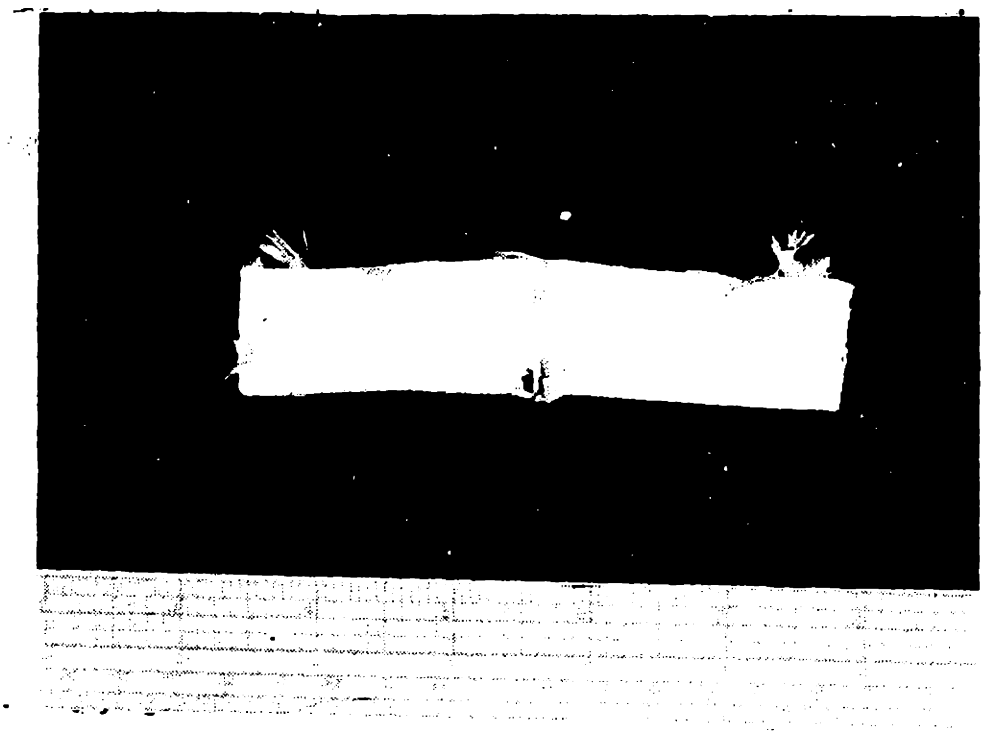

B. Notched

FIGURE 4.6: CHARPY TEST SPECIMENS

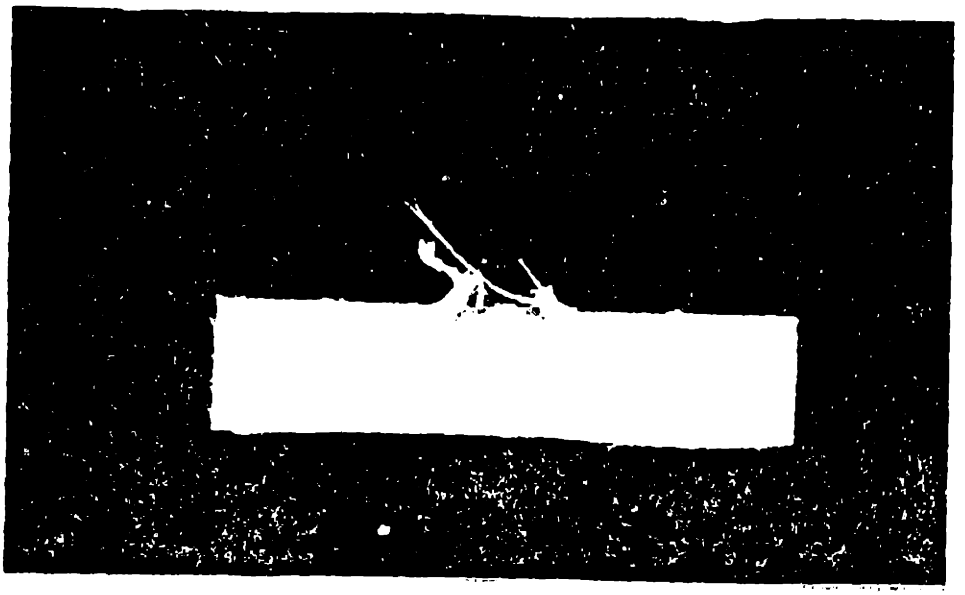

A. Unnotched

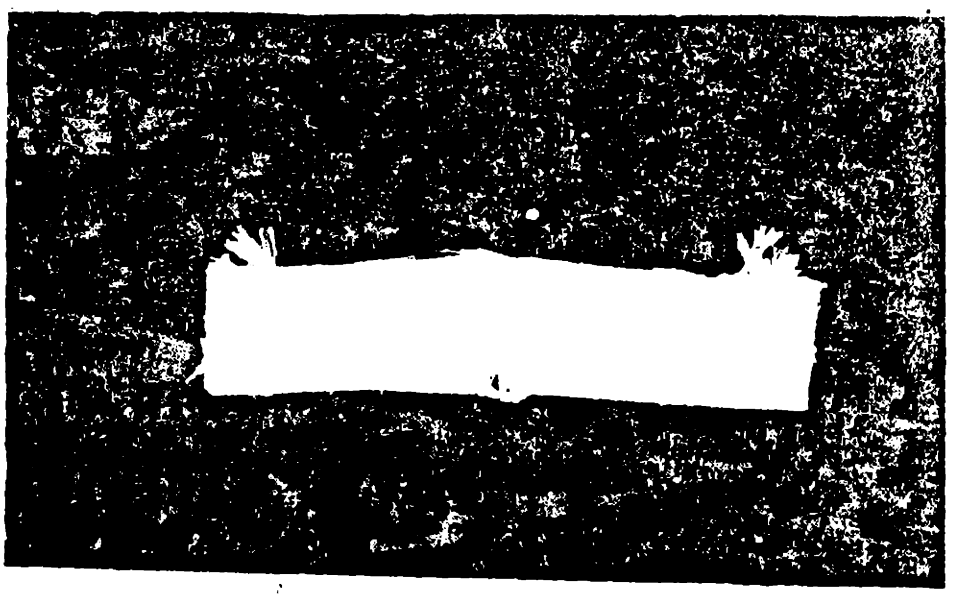

B. Notched

FIG[illegible] 4.3: CHARPY TEST SPECIMENS

V. DISCUSSION

5.1 Three-Ply Glass Yarn Composites

The composites with three-ply glass yarn showed an increase in energy absorption of 175% with increased coating thickness. Data measured from the composites with greatest energy absorption is used in the following analysis, except where otherwise noted, to correlate the theoretical analysis with experimental results.

5.1.1 Plastic Deformation and Fracture. Energy absorbed in deformation and fracture of the composite is given by Equation 2.1 as

$$W_p = \int \tau_y \, \gamma \, dV$$

where

$$\tau_y = \tfrac{1}{2} \left[\sigma_f V_f + \sigma_m' \, (1-V_f) \right] \qquad (5.1)$$

and σ_f and σ_m' are material properties. Owens-Corning gives σ_f for their yarn as 6.9×10^8 N/m^2. VanKrevelen[9] gives σ_m' for high-density polyethylene as 3×10^7 N/m^2. Fiber volume fraction was determined by weighing a 10 cm square x 0.6 cm thick sample, calculating its density and taking the density of glass as 2.54 g/cc and the density of HDPE as 0.94 g/cc, calculating the volume percentage of each. Fiber volume fraction is calculated as about 10% by this method. Tested samples showed a shear strain deformation angle estimated to be constant at

0.305 radians over a volume with conical geometry of 1.79 x 10^{-4} cm^3, as shown in Figure 5.1. Substituting these values into Equation 5.1 gives a plastic work term

$$W_p = 23.99 \text{ J}$$

This figure is within 5% of the total energy absorbed by the composite with uncoated fibers. In that sample, the shear strain is approximately 0.343 radians, and deformed volume is .280 cm^3; giving an estimated energy absorption of 28.81 J.

5.1.2 Bullet Deformation. Energy absorbed in plastic deformation of the bullet is, from Equation 2.2,

$$W_b = \int \sigma_b \varepsilon_b \, dV_b \qquad (5.2)$$

The yield strength of sand cast lead for ammunition is given by Suh and Turner[10] as 0.8 ksi. The strain measured from the test results, as indicated in Figure 5.2, varies from 0.61 to 1.20. The measured deformation volume is 0.1148 cm^3. These values, substituted into Equation 5.2, give an average energy absorption of 0.583 J, which is insignificant when compared with total energy absorption.

5.1.3 Fiber Elongation and Fluid Shear. Assuming the fibers within the deformed volume of the composite are pinned at the periphery of the deformation zone and strained to their ultimate elongation, an average length of fiber of 9.21 x 10^{-3}m over 12 layers of fibers spaced 11.3 to the

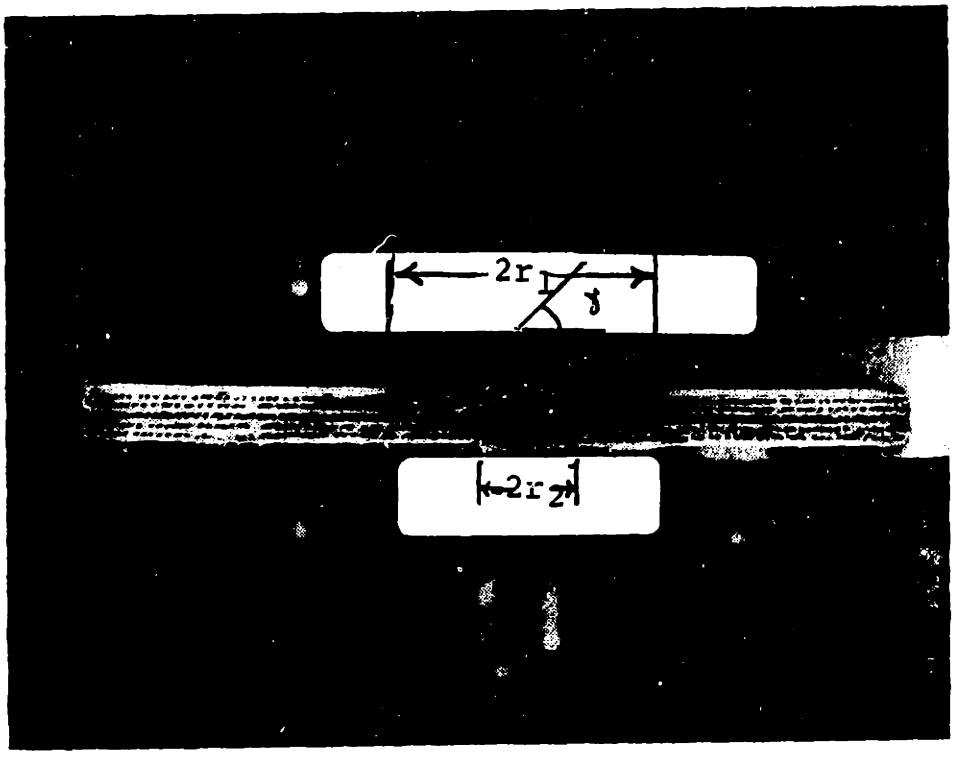

Deformed Volume $V = \frac{1}{3} h [r_1^2 + r_2^2 + r_1 r_2]$

FIGURE 5.1: COMPOSITE AFTER PERFORATION
CROSS SECTIONAL VIEW

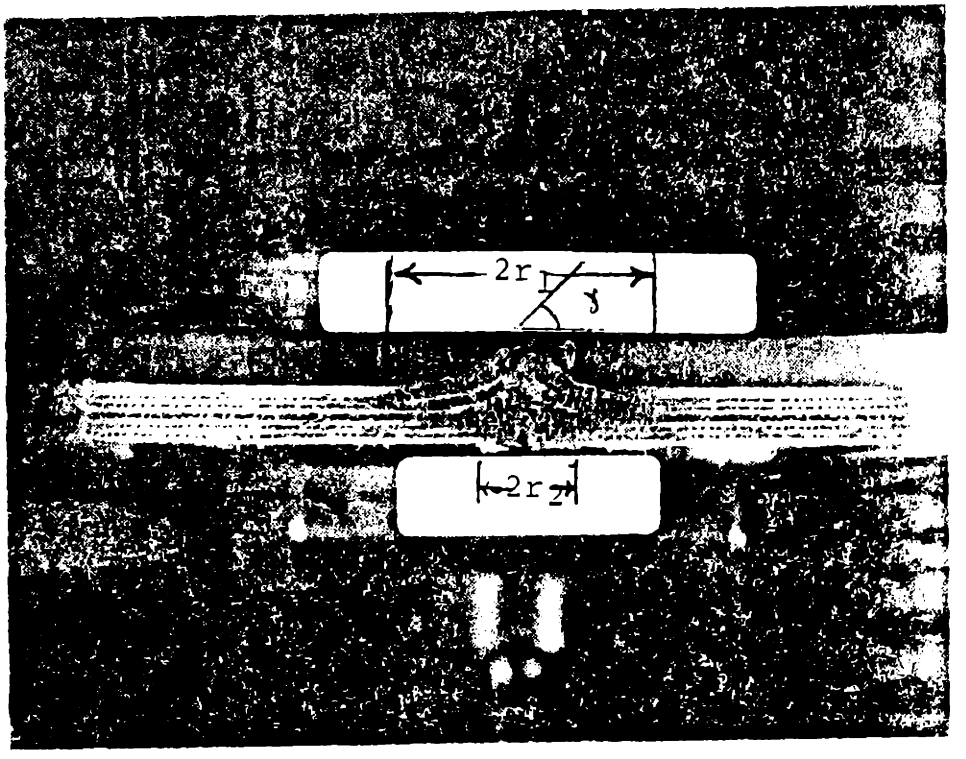

Deformed Volume $V = \frac{1}{3} h [r_1^2 + r_2^2 + r_1 r_2]$

FIGURE 5.1: COMPOSITE AFTER PERFORATION
CROSS SECTIONAL VIEW

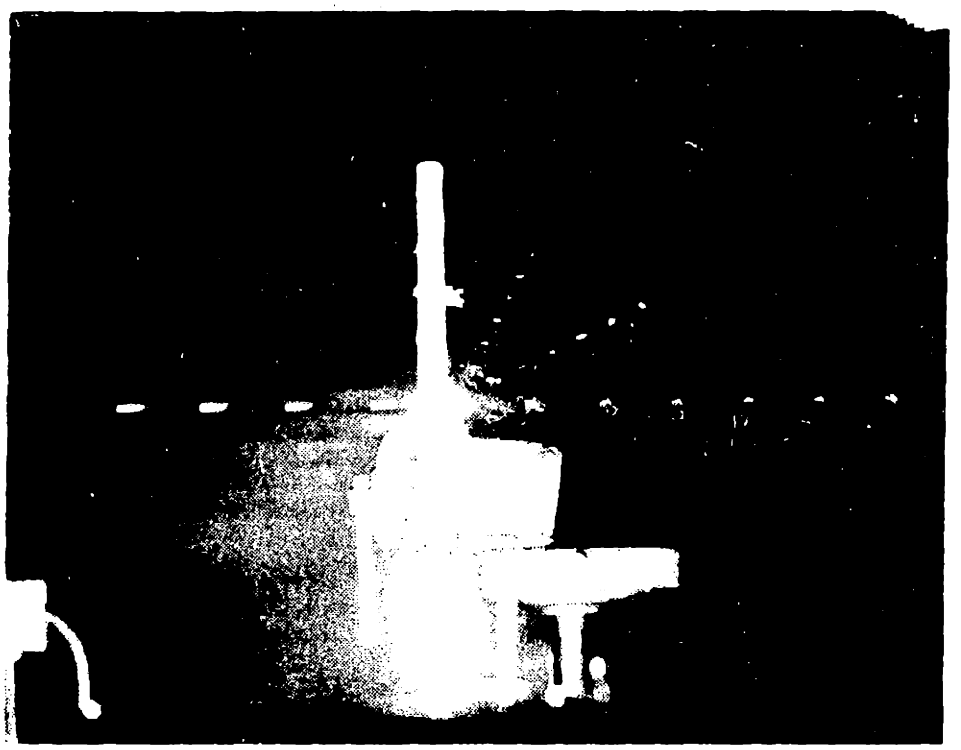

FIGURE 5.2: MULTIPLE MICROFLASH PHOTOGRAPH SHOWING BULLET DEFORMATION

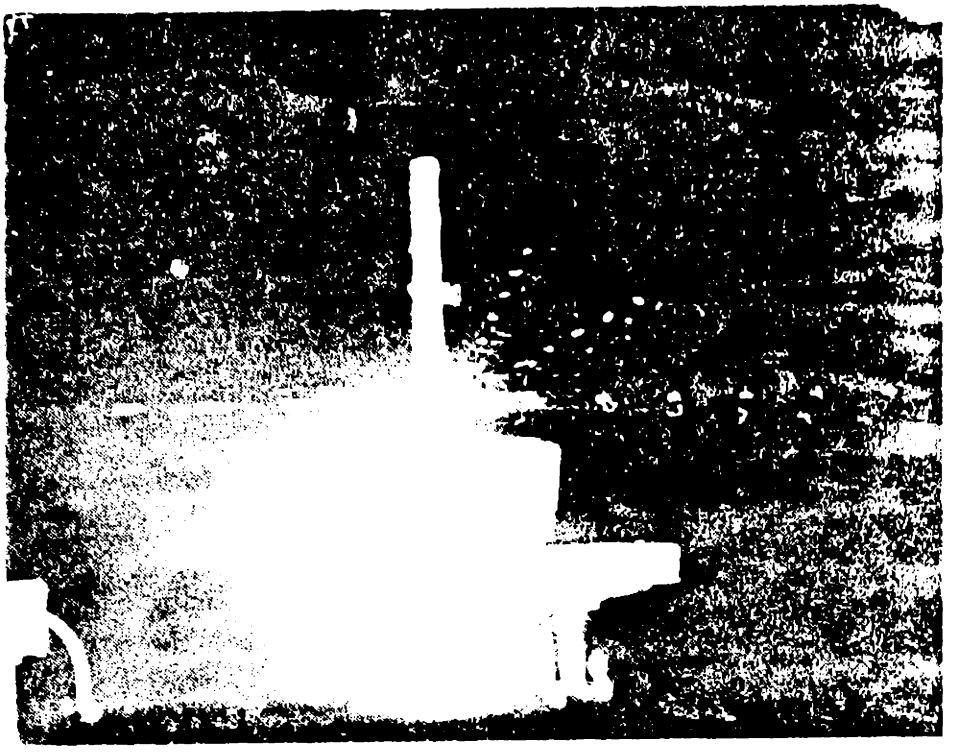

FIGURE 5.2: MULTIPLE MICROFLASH PHOTOGRAPH SHOWING BULLET DEFORMATION

centimeter is strained by 4.8% for a total fiber elongation of 5.39×10^{-2}m. The energy absorbed in shearing the fluid coating can be estimated as

$$W_s = \int \mu \frac{dV}{dR} \, dA \, dl \qquad (5.3)$$

where

$\frac{dV}{dR}$ = shear strain rate $\simeq \frac{V}{2t}$ where $\frac{V}{2}$ = average fiber velocity

V = bullet velocity = 350 m/sec

t = coating thickness

μ = fluid viscosity = .10 m/sec (10^5cs)

dA = surface area of fiber = $2\pi r\ell$

dl = total fiber elongation

The coating thickness can be estimated from the measured weight gain per unit length of yarn assuming a circular cross-section. In terms of weight per unit length W, fluid density ρ, fiber radius r, and coating thickness t,

$$W = \rho A = \rho \{\pi(R+t)^2 - \pi R^2\}$$

Solving for t gives

$$t = \sqrt{R^2 + \frac{W}{\pi\rho}} - R \qquad (5.4)$$

In the case of maximum energy absorption, $t = 7.998 \times 10^{-3}$cm. Equation 5.3 then gives

$$W_s = 256.57 \text{ Joules}$$

This value is much greater than the total energy absorbed. Errors in estimating shear stress and fiber elongation are believed to be the cause.

Shear stress is the product of fluid viscosity and strain rate. The strain rate approximation using bullet velocity and coating thickness could be inadequate at high velocities and low coating thicknesses. Coating thickness is not always uniform ard is a possible source of error. Further, a constant viscosity was assumed, but viscosity does vary with strain rate, and fluid behavior at the strain rates encountered herein is not fully understood. These possible sources of error indicate an inaccurate approximation, yet also indicate possible areas in which energy absorption may increase.

5.1.4 Inertia and Friction Effects. The dynamic work term for inertia effects for a thin plate perforated by an ogival projectile is from Chapter II.

$$W_d = 1.86\ \rho\ (\frac{VR}{L})^2\ \pi\ h_0 R^2 \qquad (5.5)$$

where

ρ = plate density = 0.94 g/cc

V = bullet velocity = 350 m/sec

R = bullet radius = 0.254 cm

L = bullet nose length = 0.5 cm

h_0 = plate thickness = 0.635 cm

in which case we have

$$W_d = 7.11 \times 10^{-5} \text{ Joules}$$

This is negligible compared to total energy absorption.

Similarly for friction we have

$$W_f = \int f\sigma_y\ A\ dl$$

where

f = friction coefficient

σ_y = material yield stress = 3×10^7 N/m^2

A = surface area between bullet and plate = $2\pi r h_0$

l = length of bullet = 0.9 cm

Assuming a maximum friction coefficient of 0.5,

W_f = 13.68 Joules

This represents 18% of the total energy absorbed. It does not vary significantly over the range of samples tested.

5.1.5 Summary. The previous discussion shows that energy absorption in plastic deformation of the composite and the bullet, and inertia and friction effects are fairly constant over the range of samples tested, with energy absorbed in fluid shear increasing with coating thickness. Plastic deformation of the composite absorbs approximately one-third of the energy in the most energy-absorbing composite. Because fibers were not pulled out of the composite with the bullet, it was unclear why the energy absorption increased. Composites with triple strand glass fibers were made and tested to examine the effects of fiber twist and elasticity upon energy absorption.

5.2 Triple Strand Glass Fibers

Owens-Corning ECG 75 1/0 glass fibers were supplied as single strand fibers with 0.7 TPI. Three strands of the fibers were used together, a triple strand fiber without twist. The

spacing between fiber bundles was increased to prevent adjacent fibers from touching, though the fiber diameter would have been nearly the same as the three-ply yarn had the triple strand bundles remained nearly circular in cross section. Comparison between triple strand and 3-ply yarn composites must, therefore, consider the difference between fiber volume fraction. Comparisons within each group of composites is possible, however.

The effect on energy absorption of the difference in fiber volume fraction between the composites with 3-ply glass yarn and those with triple strand glass fibers is minor. The composite strength as given by Equation 2.1 is 98.5 MN/m^2 for the composite with 10% 3-ply glass yarn, and 64.3 MN/m^2 for that with 5% triple strand glass, but the energy absorption with uncoated fibers is approximately the same. The energy absorption of composites with triple strand glass fibers did increase with increased coating thickness, but not as much as did that of the 3-ply glass yarn composites. The twisting of the fibers is believed to allow more elongation and movement of the fibers within the fluid as they elongate and untwist. The resulting increase in fluid shear increases the energy absorption of the composite.

5.3 Kevlar Fibers

Kevlar fibers are said by DuPont to have a tensile strength four times that of glass fibers, 2760 MN/m^2 (400 ksi). Tensile tests conducted in association with this work, however,

measured the tensile strength of Kevlar 49 at 1339 MN/m^3 (194 ksi). The elastic moduli of the two fibers were measured as 36,570 and 38,640 MN/m^2 (5.3 and 5.6 x 10^6 psi) whereas DuPont gives them as 124,000 and 58,500 MN/m^2 (18 and 8.5 x 10^6 psi), respectively. The failure of the composites with Kevlar fibers to show the expected increased in strength and plastic deformation over the composites with glass fibers might be because of this discrepancy in tensile strength and modulus of the fibers. The small increase in energy absorption with fluid coating is partially because of the poor wetting of the fibers by the fluid, and the resulting non-uniform coating.

5.4 Summary

The tensile strength of the fibers has been shown to have little effect on the ballistic impact resistance/energy absorption of the fiber-matrix system at fiber volume fractions of 5-10%. The composites with fibers with higher elongations-to-break showed greater increases in energy absorption with increased coating thicknesses in the cases of both glass and Kevlar fibeers. Three-ply glass yarn composites showed an increase energy absorption with coating thickness of 175%, compared with 50% for triple strand glass fiber composites; Kevlar 29 composites showed an increase of 65%, compared with 57% for Kevlar 49 composites. It is clear that the most dramatic increase was shown by the 3-ply twisted yarn composites.

VI. CONCLUSIONS AND RECOMMENDATIONS

It has been demonstrated that the energy absorption of fiber-reinforced thermoplastics at high impact velocities can be increased by coating the fibers with a viscous oil. Energy absorption increased with coating thickness until the coating became excessively heavy and non-uniform. Fibers with higher elongation-to-break were shown to exhibit greater increases in energy absorption with coating thickness than were more brittle fibers. The greater elongation within the fluid increases the energy absorbed in fluid shear. A 3-ply twisted yarn demonstrated the greatest increase in energy absorption with increased coating thickness. This is believed to be caused by increased fluid shear as the fibers elongate and untwist.

An optimal relationship between fiber strength, modulus of elasticity, degree of twist, and coating thickness could likely be defined with further tests of the type described herein. An optimal configuration would probably depend as well upon the impact velocity, and could be defined in terms of that parameter. It is recommended that further study be directed at defining this optimal relationship.

This work has considered only the impact velocity of a .22 caliber long rifle bullet. It is recommended that further study consider other impact velocities, particularly those encountered in automobile accidents. Such tests would

affirm the applicability of these materials to automobile parts.

The fabrication methods used in this work were very slow and tedious. If these materials are to be widely used, a more efficient methods of producing them needs to be determined. It is recommended that further study investigate means of producing coated fiber-reinforced thermoplastics in sheet form and of thermoforming them into finished parts.

REFERENCES

[1]Marston, T.U., Atkins, A.G., and Felbeck, D.K., "Interfacial Fracture Energy and the Toughness of Composites," J. Materials Science, 9, 447-55, 1974.

[2]Millman, R.S. and Morley, J.G., "Energy Absorption at High Rates of Deformation in Fibrous Composites with Non-Fracturing Reinforcing Elements," Materials Science and Engineering, 23, 1976, pp. 1-10.

[3]Favre, J.P., "Improving the Fracture Energy of Carbon Fibre-Reinforced Plastics by Delamination Promoters," J. Materials Science, 12, 1977, pp. 43-50.

[4]Jones, T.J., "A Method of Improving the Fracture Toughness of Fiber-Reinforced Composites," S.M. Thesis, M.I.T., January 1976.

[5]Ibid., p. 53.

[6]Goldsmith, W., Impact, Edward Arnold Ltd., 1960.

[7]Awerbuch, J. and Bodner, S.R., "Analysis of the Mechanics of Perforation of Projectiles in Metallic Plates," Int. J. Solid Structures, 10, 1974, pp. 671-684.

[8]Goldsmith, op. cit., p. 244.

[9]"Information About Silicone Fluids," Dow-Corning Corp., Midland, MI.

[10]Jones, T.J., op. cit., p. 69.

[11]Van Krevelen, Properties of Polymers, 2nd Edition, Elsevier Press, 1976, p. 303.

[12]"Textile Fibers for Industry," Owens-Corning Fiberglas Corp., Pub. No. S-TUD-8285, Feb. 1979.

[13]"Characteristics and Uses of Kevlar® 49 Aramid High Modulus Organic Fiber," DuPont Technical Information Bulletin K-2, February 1978.

[14]"Characteristics and Uses of Kevlar® 29 Aramid," DuPont Preliminary Information Memo, No. 375, September 28, 1976.

[15]Van Krevelen, op. cit., p. 303.

[16]Suh, N.P. and Turner, A.P.L., Elements of the Mechanical Behavior of Solids, McGraw-Hill, 1975, p. 597.